

## Appendix

This Appendix presents the measured strains, critical temperatures, coercive fields, and critical fields of the b-axis-oriented Dy samples used in this research. These values are contained in Table A.1. It also contains the measured hysteresis loops for the samples, which appear as Figures A.1 through A.12 on the subsequent pages. Finally, this Appendix contains hysteresis loops for the samples in the antiferromagnetic state, which demonstrate the temperature-independence of the critical field,  $H_C$ .

Sample	%Y content	$\epsilon_{11}$ (%)	$\epsilon_{22}$ (%)	$\epsilon_{33}$ (%)	T <sub>C</sub> (K)	H <sub>CO</sub> (Oe)	H <sub>C</sub> (kOe)
DY20	0	-2.24	1.15	-1.89	145	7.44	16.1
DY15B	16	-1.66	0.86	-1.43	135	7.03	14.0
DY17	28	-1.23	0.64	-1.08	110	5.09	12.0
DY13	40	-0.80	0.42	-0.73	97	5.10	12.0
DY33	64	0.06	-0.01	-0.03	78	2.20	11.0
DY14	75	0.50	-0.23	0.32	90	1.93	9.6
DY32	77	0.53	-0.25	0.35	115	2.47	7.9
DY26A	80	0.64	-0.30	0.43	135	2.47	7.0
DY26D	82	0.71	-0.34	0.49	140	2.03	n.a.
DY35	87	0.89	-0.43	0.64	145	2.89	n.a.
DY36F	95	1.18	-0.58	0.87	154	2.85	n.a.
DY23	100	1.36	-0.67	1.01	165	2.37	n.a.

Table A.1. The strains, critical temperatures, coercive fields and critical fields for the b-axis-oriented Dy samples used in this research. The percentage of Y contained in the alloy buffer layer and the in-plane strains  $\epsilon_{11}$  and  $\epsilon_{22}$  were obtained from x-ray diffraction measurements of the Y/Lu alloy buffer layers; the out-of-plane strains were calculated according to Eq. (1.8). The coercive fields are the average coercive fields obtained for increasing and decreasing applied field.

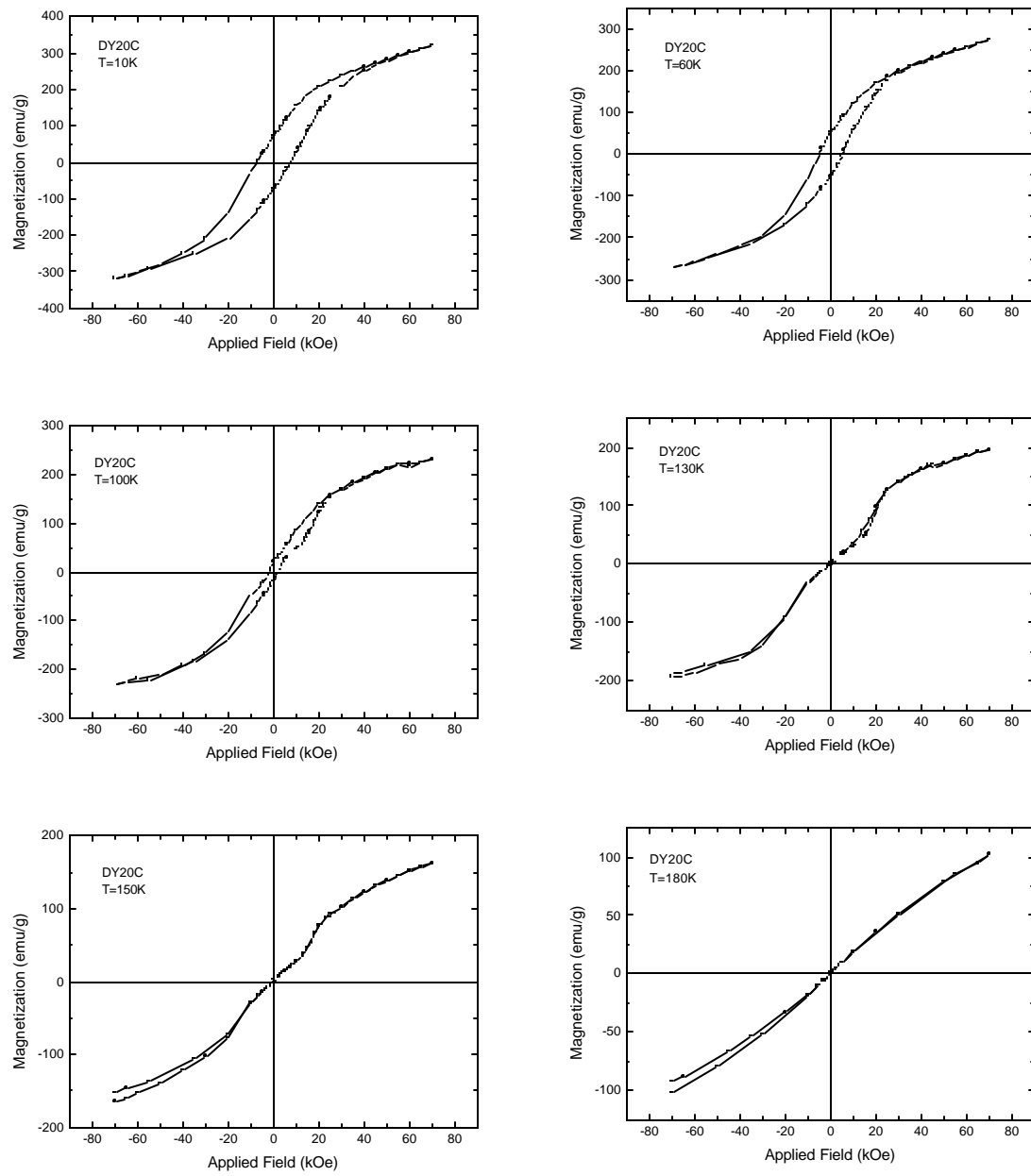


Figure A.1. Hysteresis loops for the sample DY20, with  $\epsilon_{11}=-2.24\%$ .

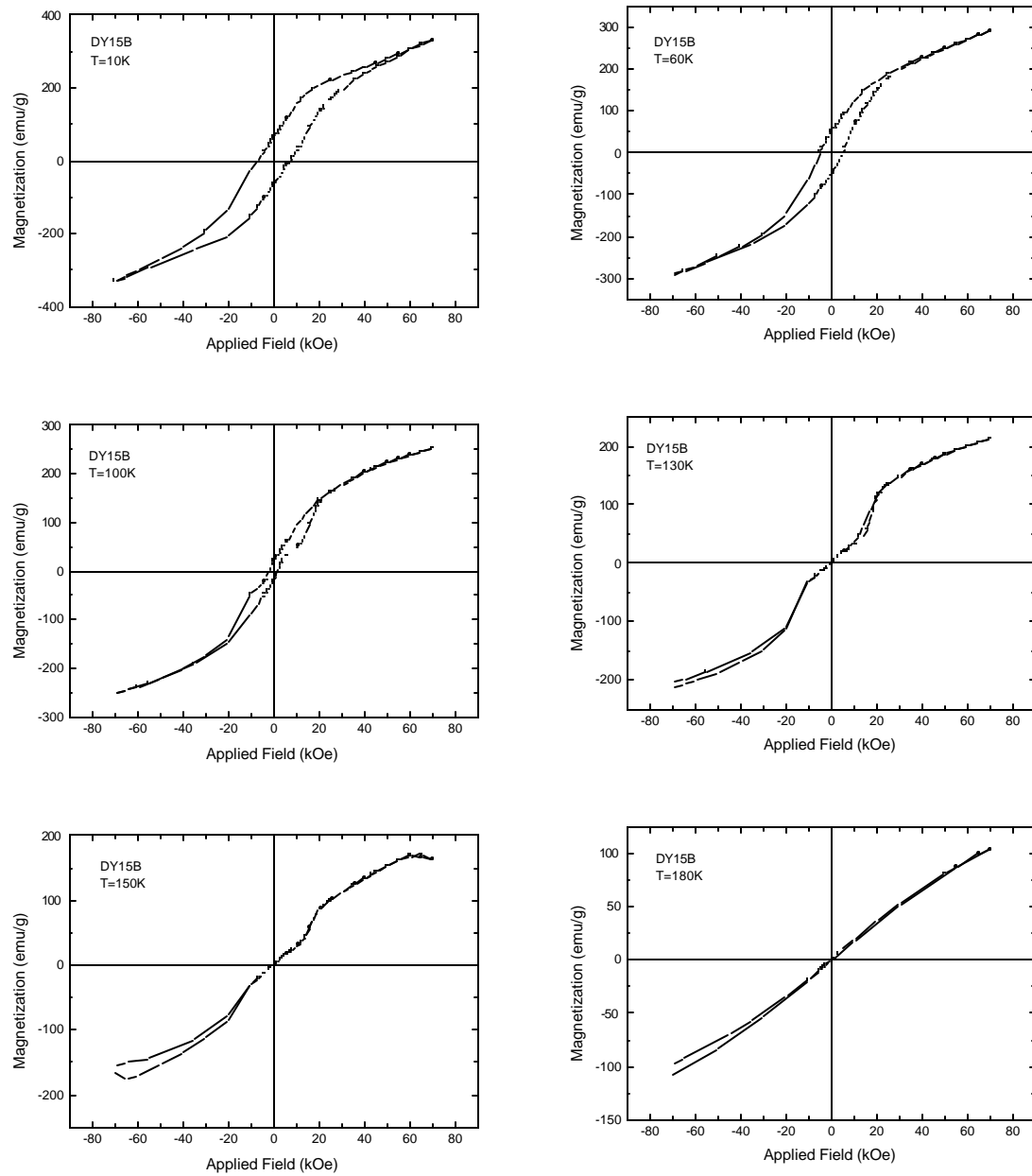


Figure A.2. Hysteresis loops for the sample DY15B, with  $\varepsilon_{11}=-1.66\%$ .

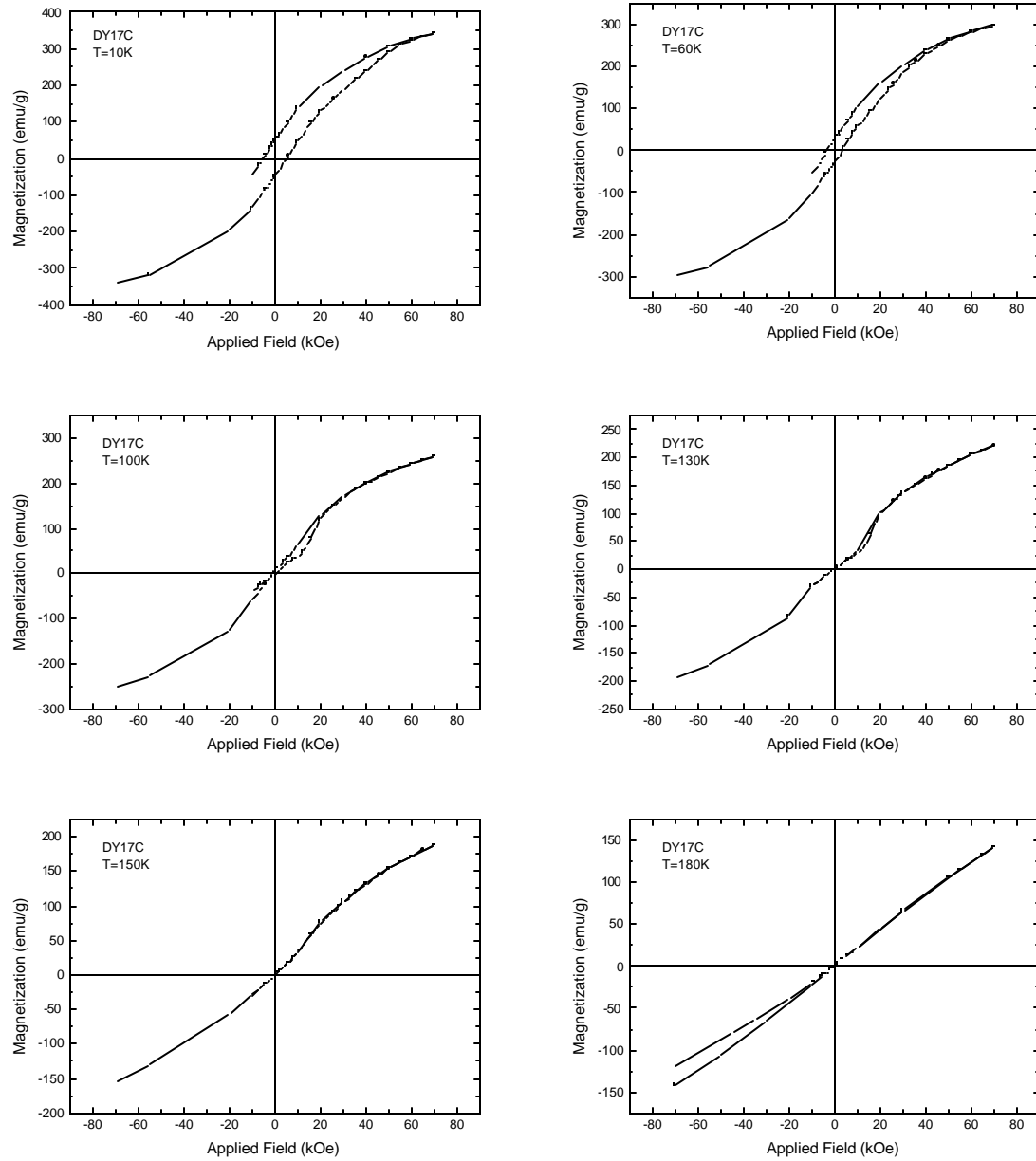


Figure A.3. Hysteresis loops for the sample DY17, with  $\epsilon_{11}=-1.23\%$ .

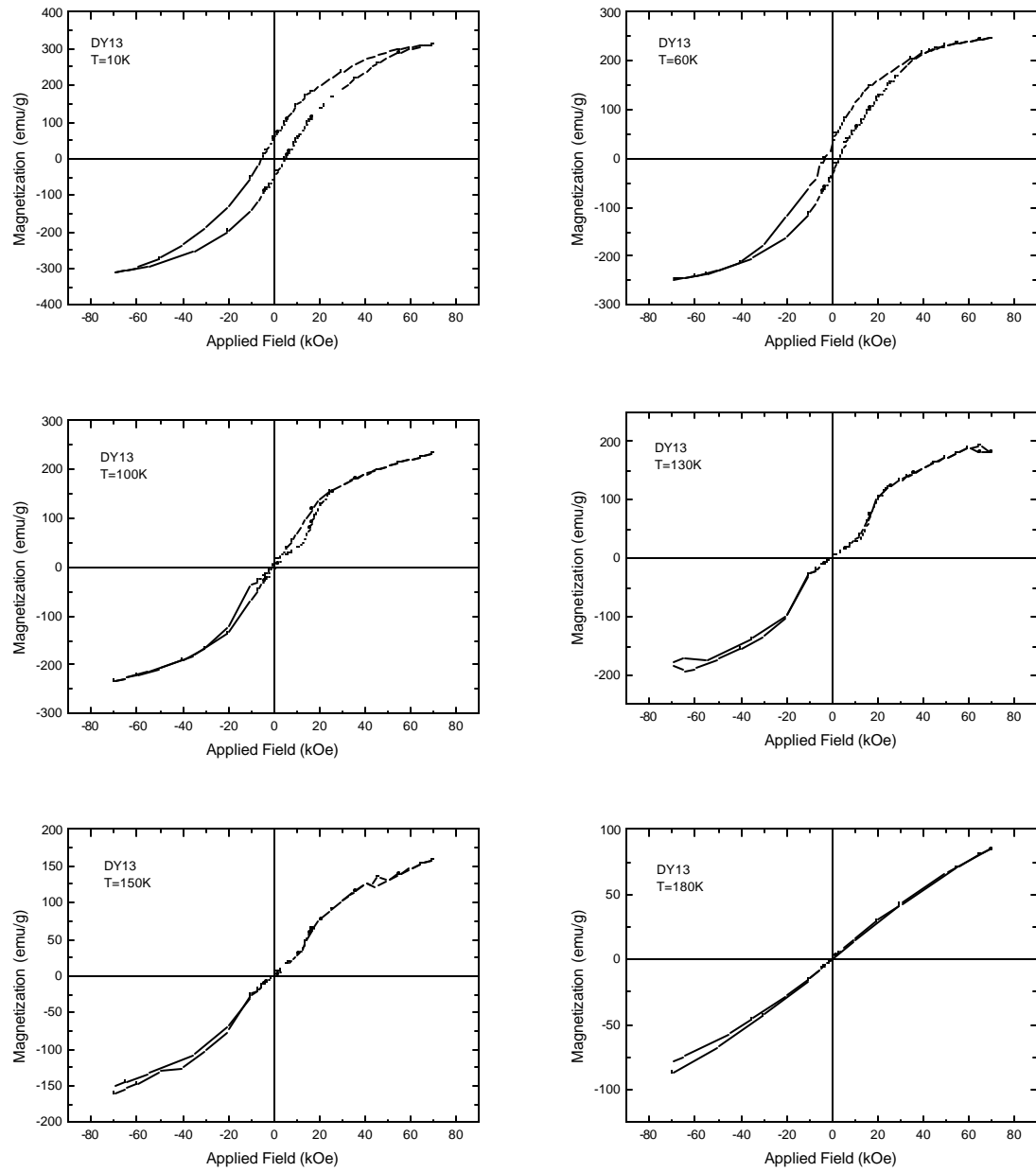


Figure A.4. Hysteresis loops for the sample DY13, with  $\epsilon_{11}=-0.88\%$ .

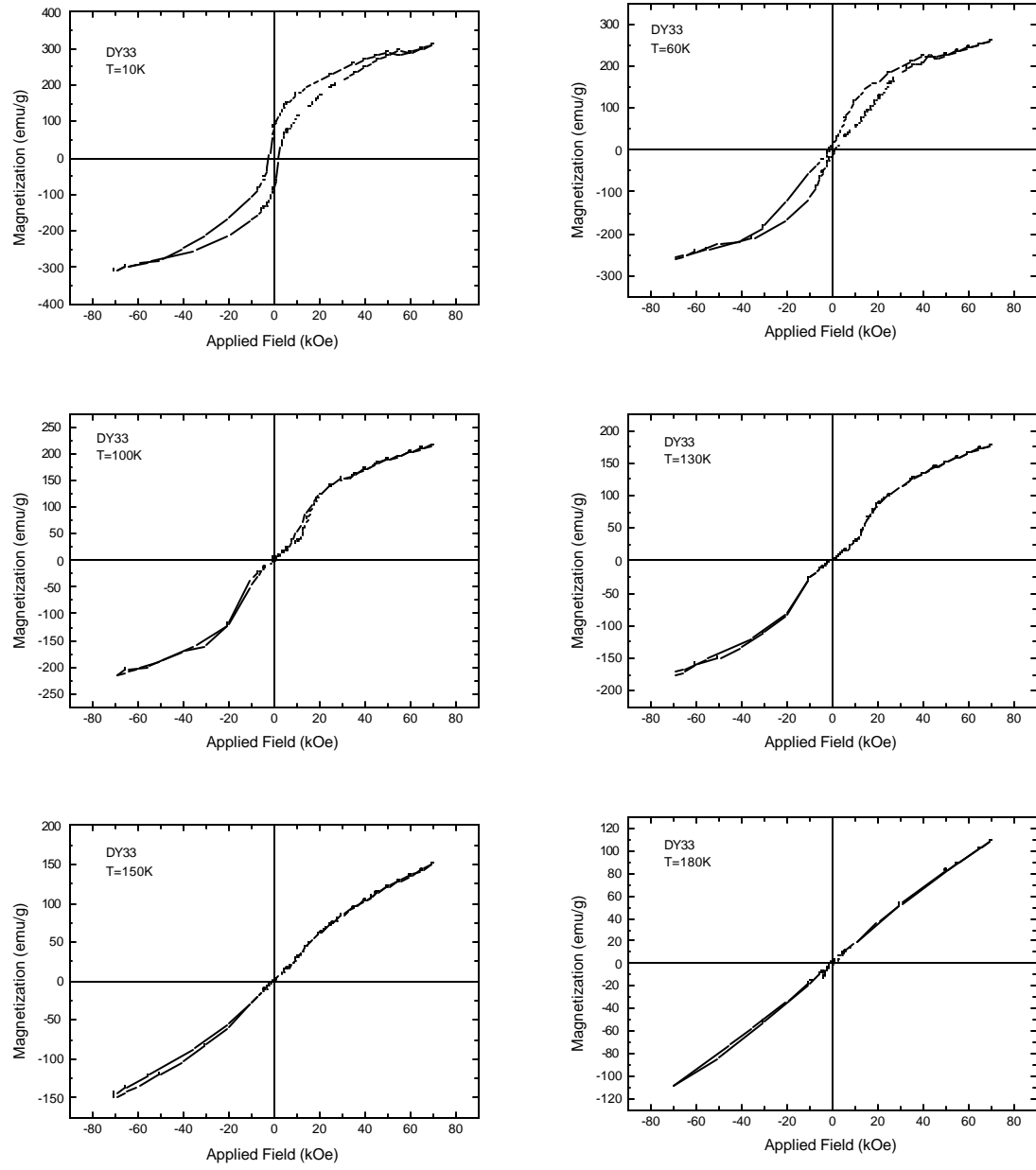


Figure A.5. Hysteresis loops for the sample DY33, with  $\epsilon_{11}=+0.06\%$ .

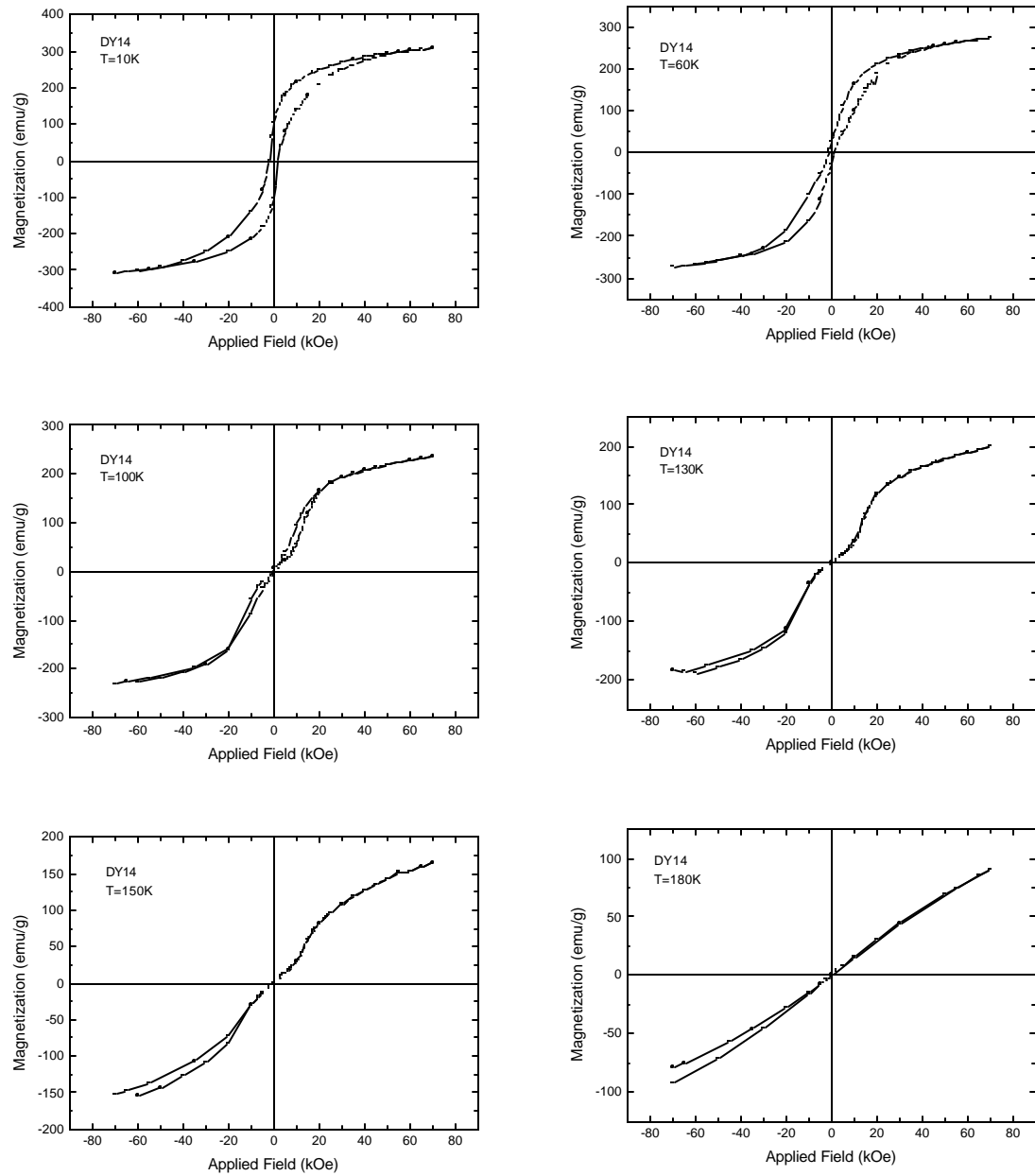


Figure A.6. Hysteresis loops for the sample DY14, with  $\varepsilon_{11}=+0.50\%$ .

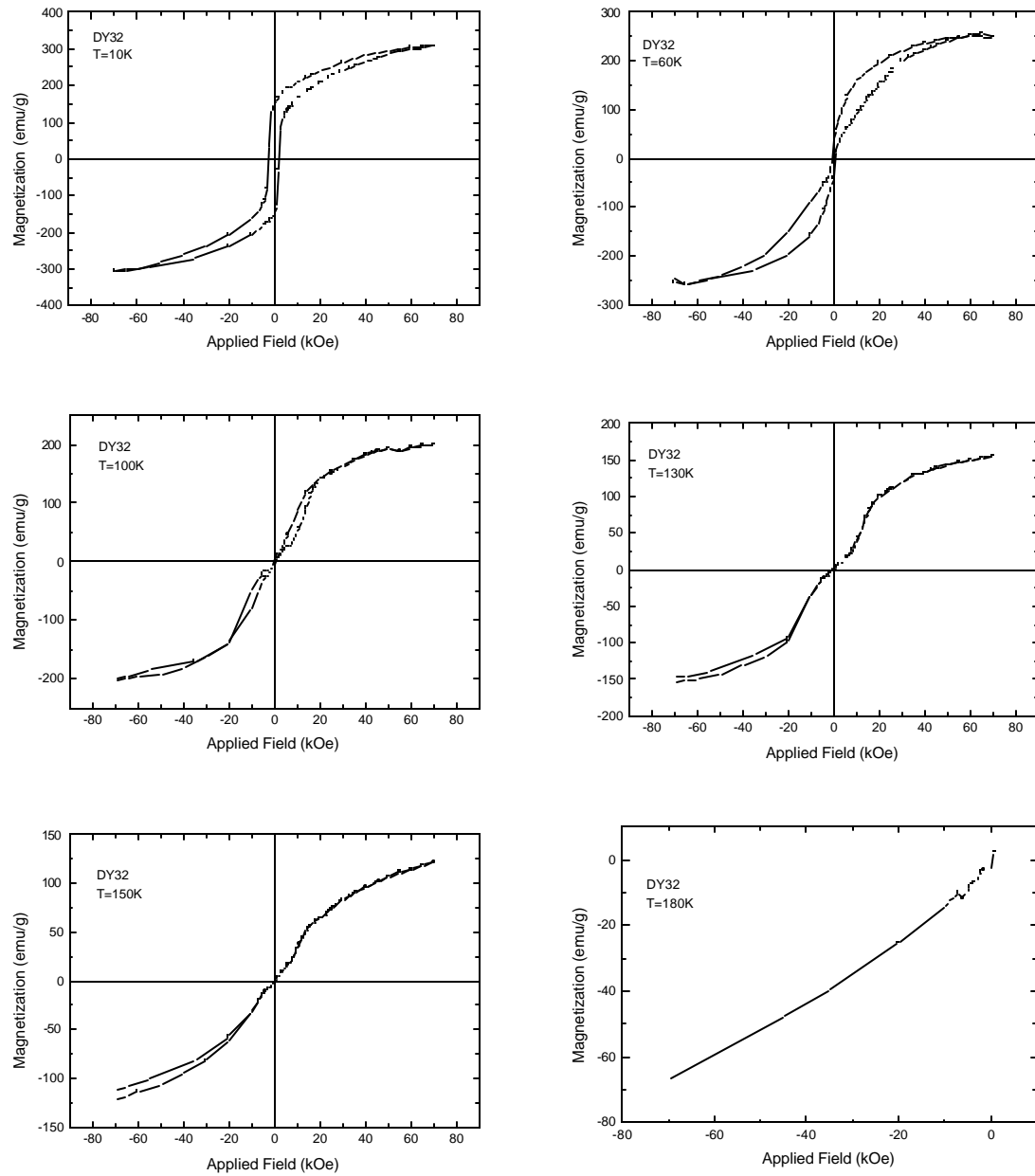


Figure A.7. Hysteresis loops for the sample DY32, with  $\varepsilon_{11}=+0.53\%$ .

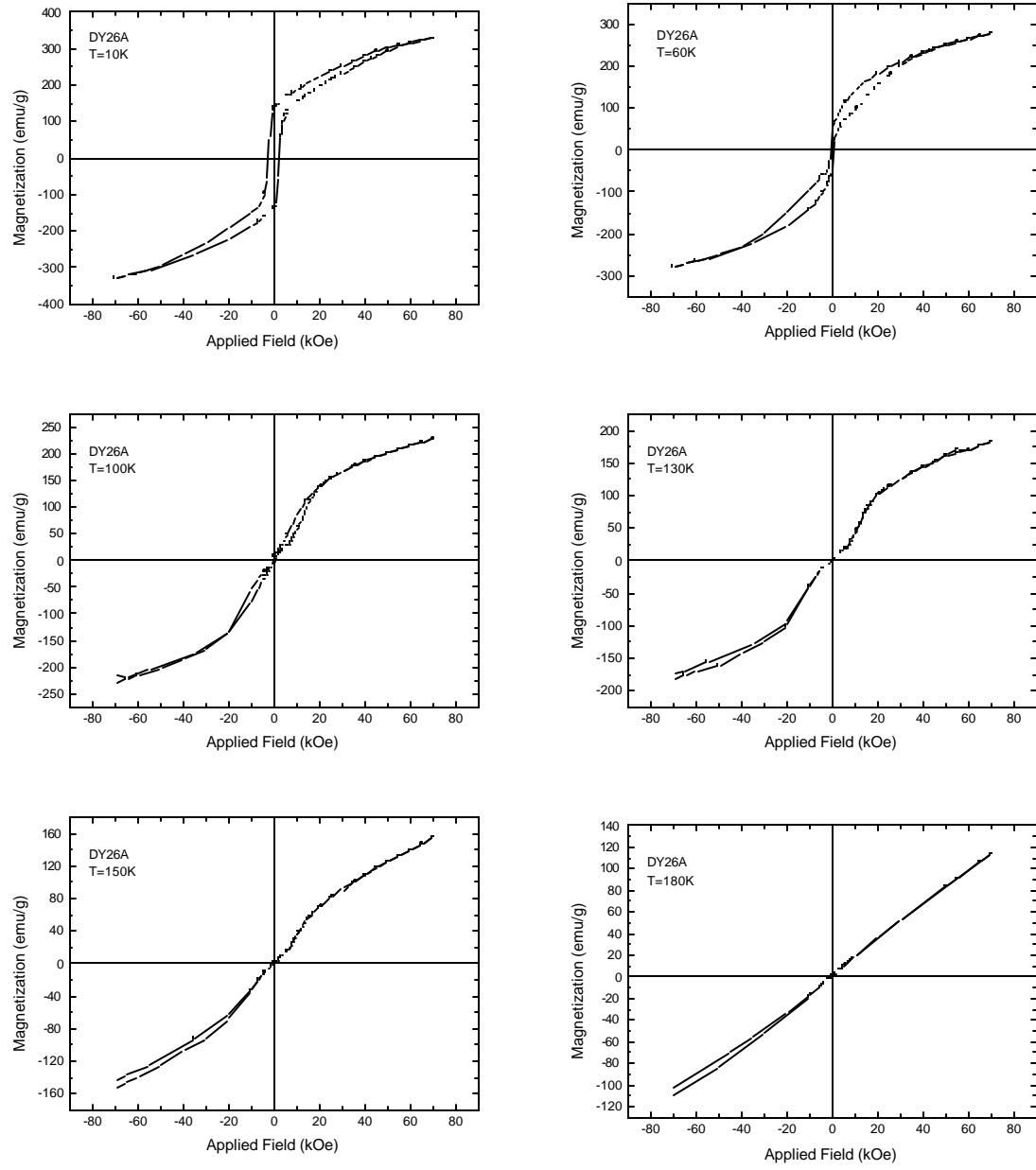


Figure A.8. Hysteresis loops for the sample DY26A, with  $\varepsilon_{11}=+0.64\%$ .

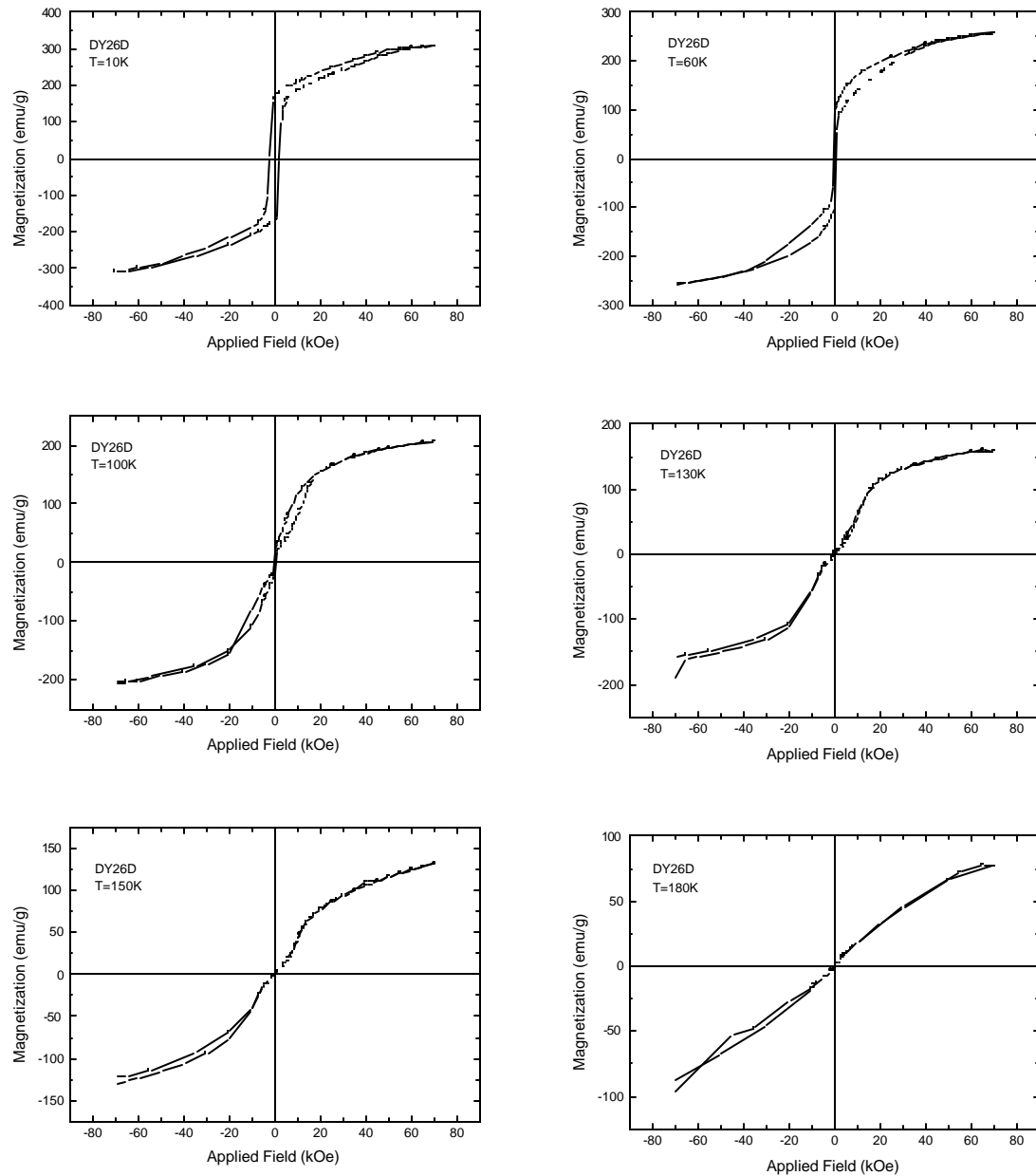


Figure A.9. Hysteresis loops for the sample DY26D, with  $\varepsilon_{11}=+0.71\%$ .

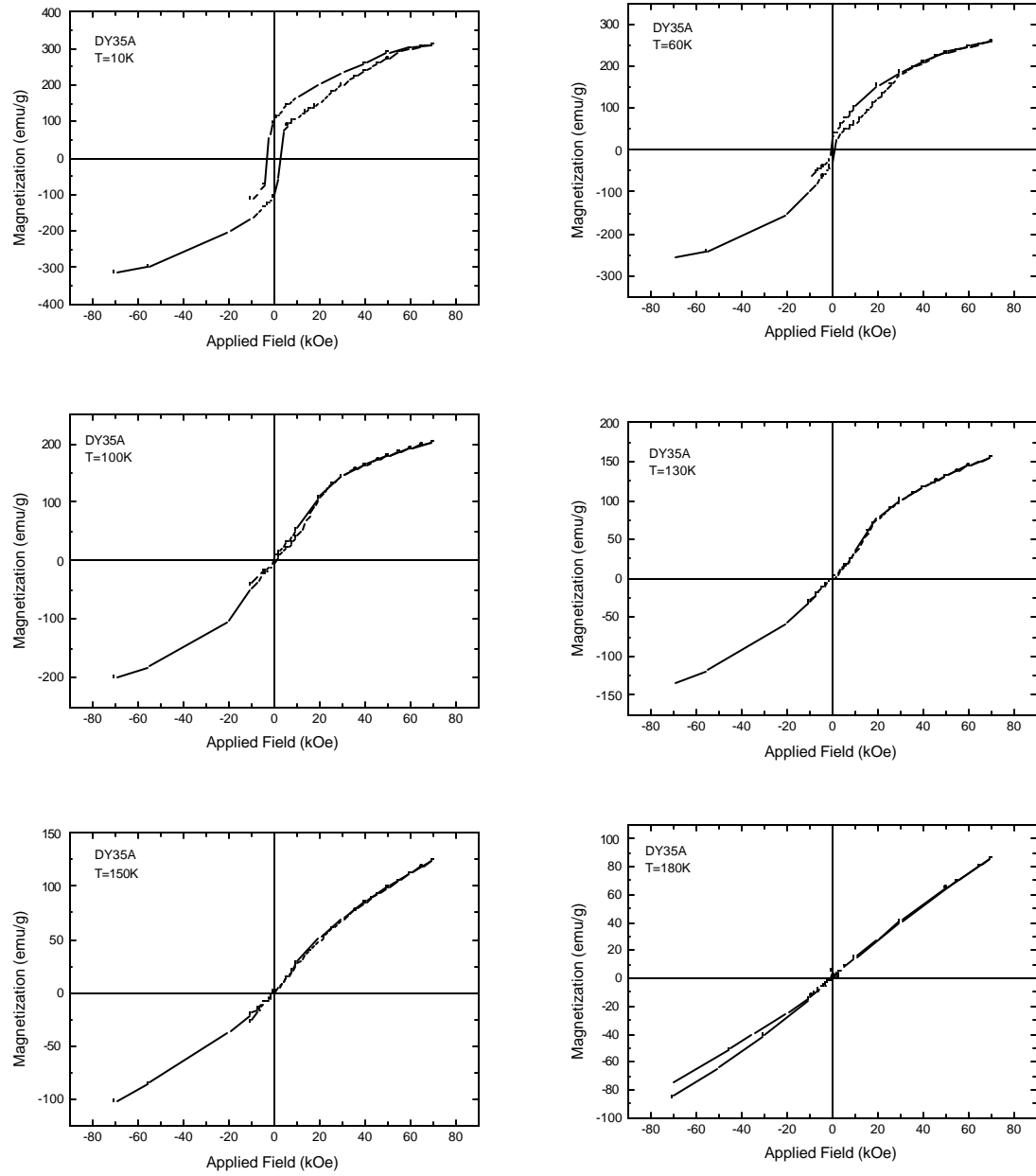


Figure A.10. Hysteresis loops for the sample DY35, with  $\varepsilon_{11}=+0.89\%$ .

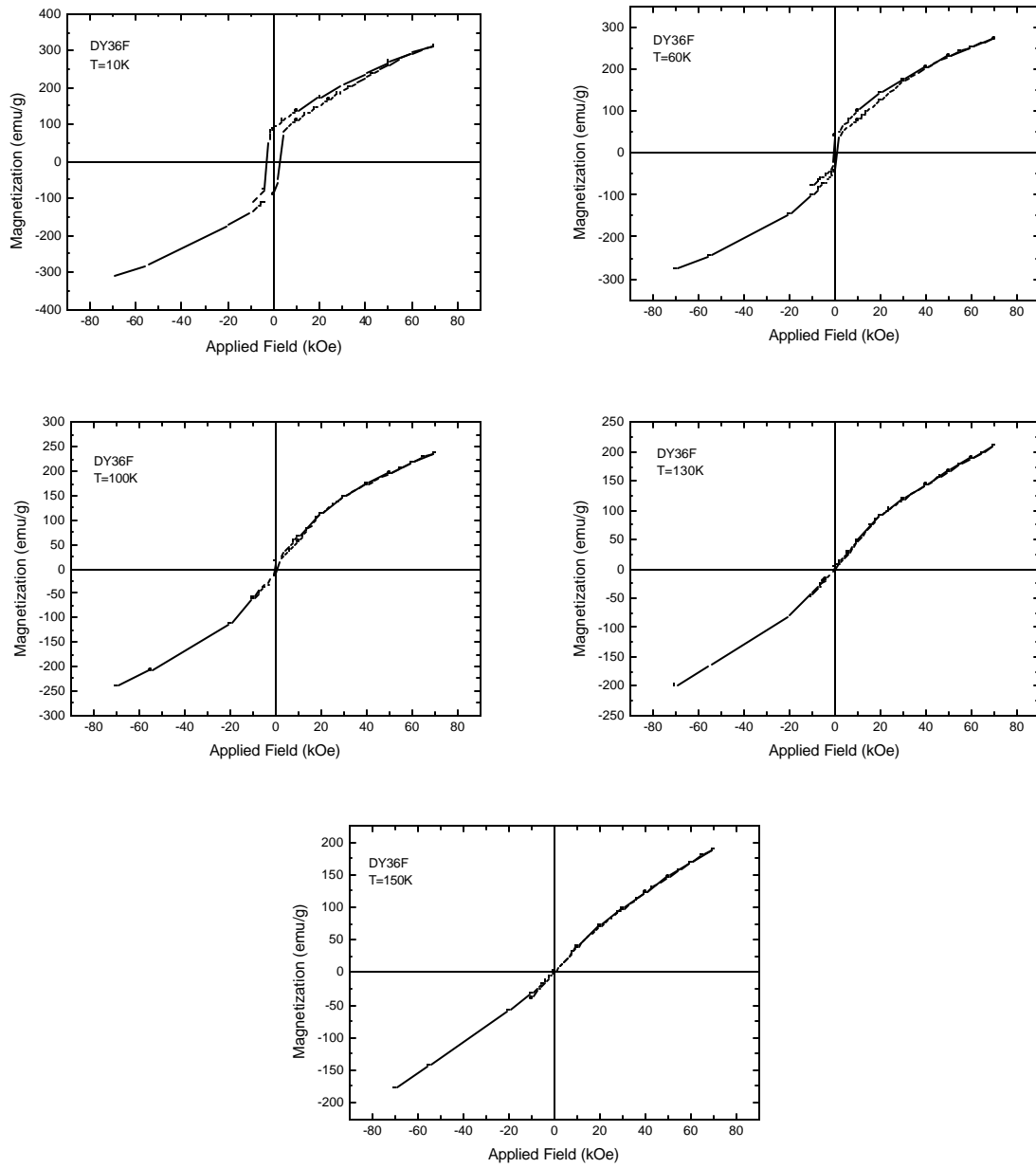


Figure A.11. Hysteresis loops for the sample DY36F, with  $\epsilon_{11}=+1.18\%$ .

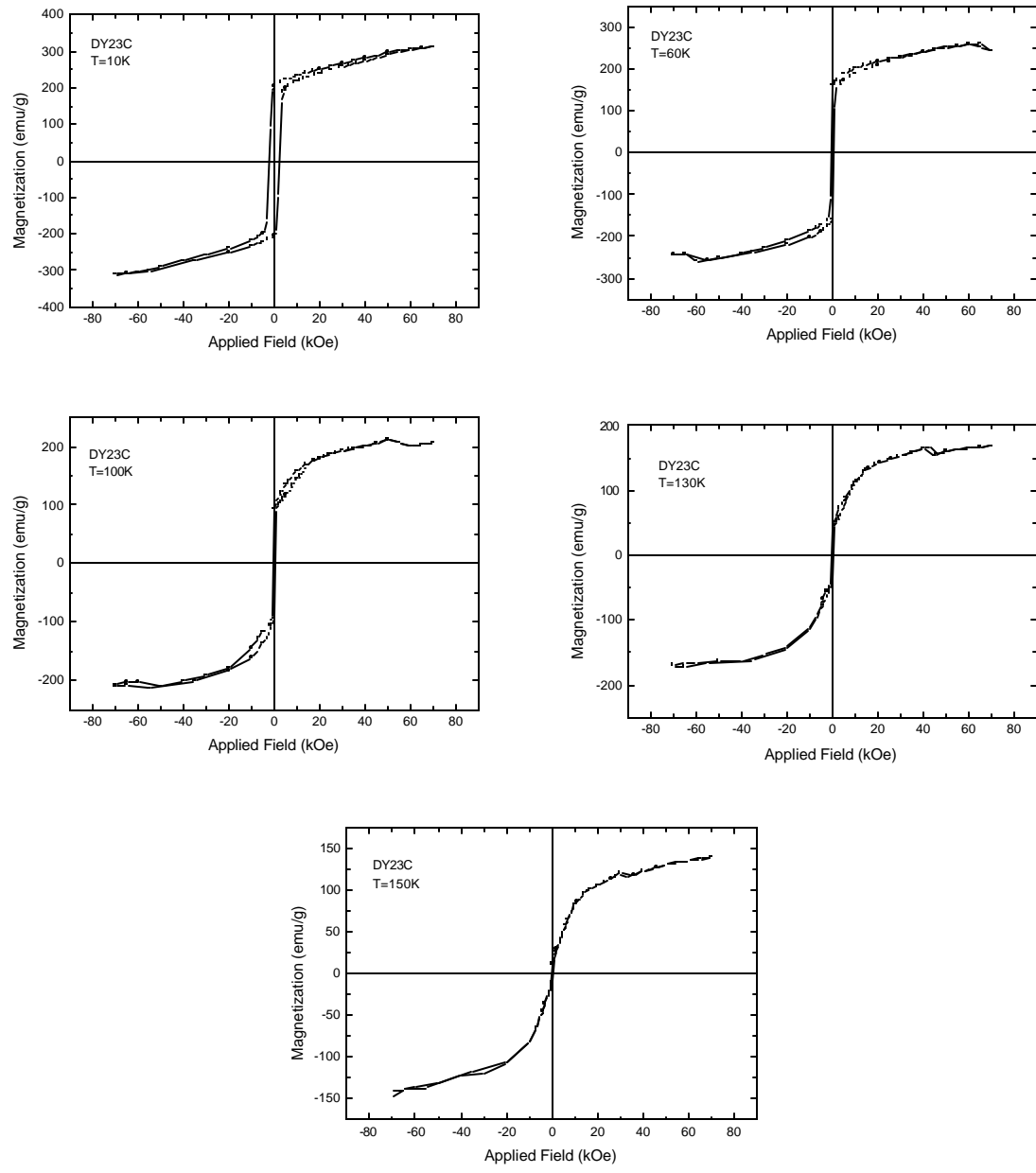


Figure A.12. Hysteresis loops for the sample DY23, with  $\epsilon_{11}=+1.36\%$ .

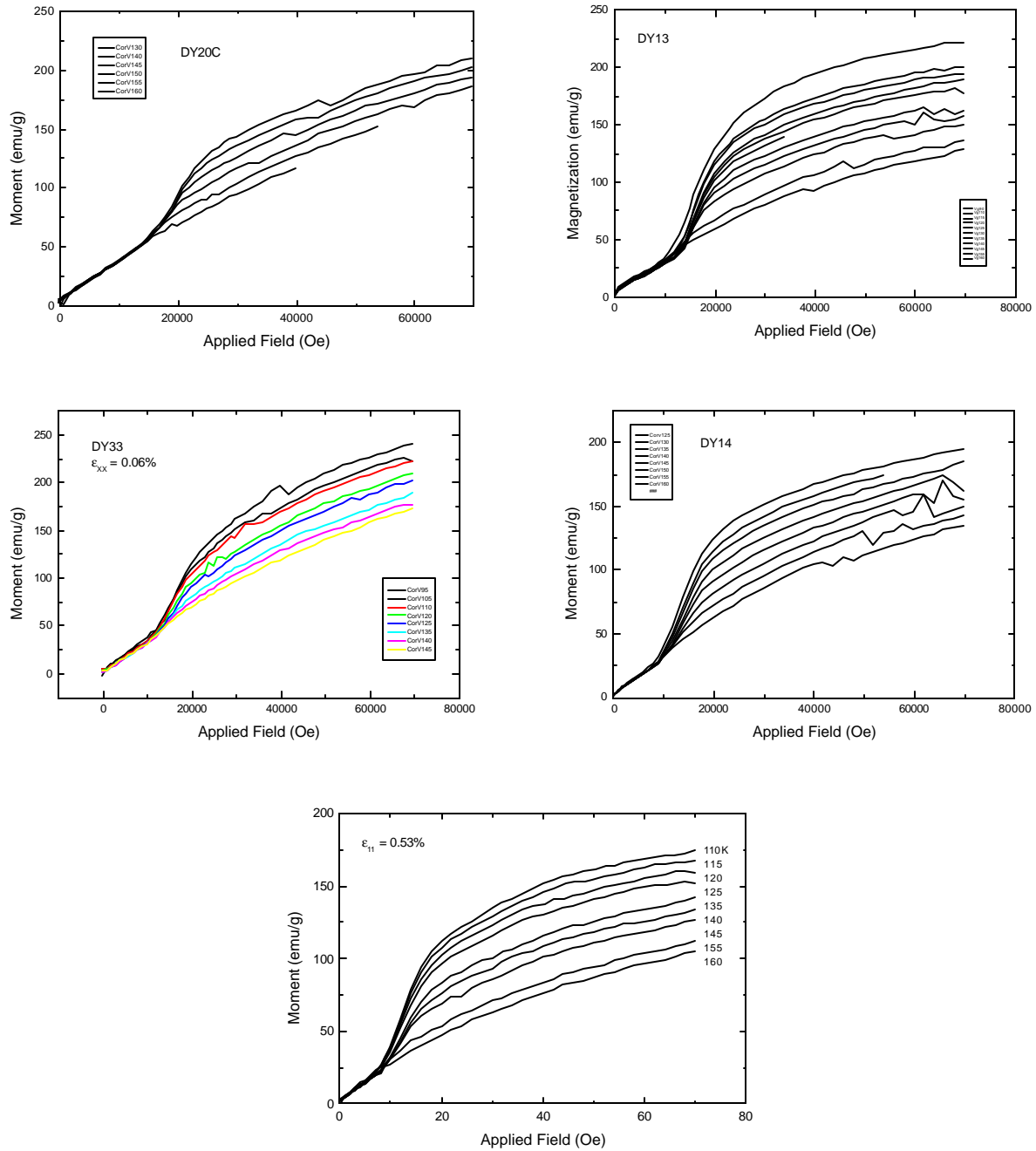


Figure A.13. Hysteresis loops for various samples in the antiferromagnetic phase, demonstrating that the critical field does not depend strongly on temperature.